MICROBIOLOGY

RESEARCH ARTICLE

Holman *et al.*, *Microbiology* 2021;167:001103

DOI 10.1099/mic.0.001103

MICROBIOLOGY SOCIETY

OPEN ACCESS

Alanine-scanning mutagenesis of protein mannosyl-transferase from *Streptomyces coelicolor* reveals strong activity-stability correlation

Nathaniel D. M. Holman[1], Anthony J. Wilkinson[2,*] and Margaret C. M. Smith[1]

Abstract

In *Actinobacteria*, protein O-mannosyl transferase (Pmt)-mediated protein O-glycosylation has an important role in cell envelope physiology. In *S. coelicolor,* defective Pmt leads to increased susceptibility to cell wall-targeting antibiotics, including vancomycin and *β*-lactams, and resistance to phage φC31. The aim of this study was to gain a deeper understanding of the structure and function of *S. coelicolor* Pmt. Sequence alignments and structural bioinformatics were used to identify target sites for an alanine-scanning mutagenesis study. Mutant alleles were introduced into *pmt*-deficient *S. coelicolor* strains using an integrative plasmid and scored for their ability to complement phage resistance and antibiotic hypersusceptibility phenotypes. Twenty-three highly conserved Pmt residues were each substituted for alanine. Six mutant alleles failed to complement the *pmt*⁻ strains in either assay. Mapping the six corresponding residues onto a homology model of the three-dimensional structure of Pmt, indicated that five are positioned close to the predicted catalytic DE motif. Further mutagenesis to produce more conservative substitutions at these six residues produced Pmts that invariably failed to complement the DT1025 *pmt*⁻ strain, indicating that strict residue conservation was necessary to preserve function. Cell fractionation and Western blotting of strains with the non-complementing *pmt* alleles revealed undetectable levels of the enzyme in either the membrane fractions or whole cell lysates. Meanwhile for all of the strains that complemented the antibiotic hypersusceptibility and phage resistance phenotypes, Pmt was readily detected in the membrane fraction. These data indicate a tight correlation between the activity of Pmt and its stability or ability to localize to the membrane.

INTRODUCTION

Protein glycosylation is a post-translational modification observed in all domains of life. The composition and structure of glycan moieties can vary greatly and their attachment to a target protein variously alters physicochemical properties, cellular localization, ligand binding, and stability [1]. Glycans are most commonly attached to serine/threonine (O-glycosylation) or asparagine (N-glycosylation) residues. Actinobacteria have a protein O-glycosylation system that resembles eukaryotic protein O-mannosylation. Two principal enzymes in this pathway are polyprenol phosphate mannose synthase (Ppm1) and protein-O-mannosyl transferase (Pmt) [2]. Ppm1 initially synthesizes a sugar donor, polyprenol phosphate mannose (PPM), by catalysing the transfer of mannose from GDP-mannose to polyprenol phosphate on the cytoplasmic face of the plasma membrane (Fig. 1). The orientation of PPM is then thought to be flipped by an unknown mechanism so that the mannose residue is located on the periplasmic side of the cytoplasmic membrane. The protein-O-mannosyl transferase (Pmt) then transfers mannose from PPM to membrane and secreted proteins in the periplasm. This pathway is conserved across the eukaryotic kingdom where dolichol phosphate rather than polyprenol phosphate serves as the mannose carrier [1].

Recent studies of the actinobacteria, *Mycobacterium tuberculosis* and *Corynebacterium glutamicum,* have shown that strains deficient in Pmt activity have growth-retarded phenotypes [3, 4]. In addition, *pmt*⁻ strains of *Streptomyces*

Received 29 July 2021; Accepted 13 September 2021; Published 22 October 2021

Author affiliations: [1]Department of Biology, University of York, York YO10 5DD, UK; [2]Structural Biology Laboratory, York Biomedical Research Institute, Department of Chemistry, University of York, York YO10 5DD, UK.

***Correspondence:** Anthony J. Wilkinson, tony.wilkinson@york.ac.uk

Keywords: antibiotic susceptibility; alanine-scanning mutagenesis; homology model; protein mannosylation; *Streptomyces coelicolor*.

Abbreviations: DN, Difco nutrient; PFU, plaque forming units; Pmt, protein O-mannosyl transferase; PPM, polyprenol phosphate mannose; SN, soft nutrient.

Six supplementary tables and ten supplementary figures are available with the online version of this article.

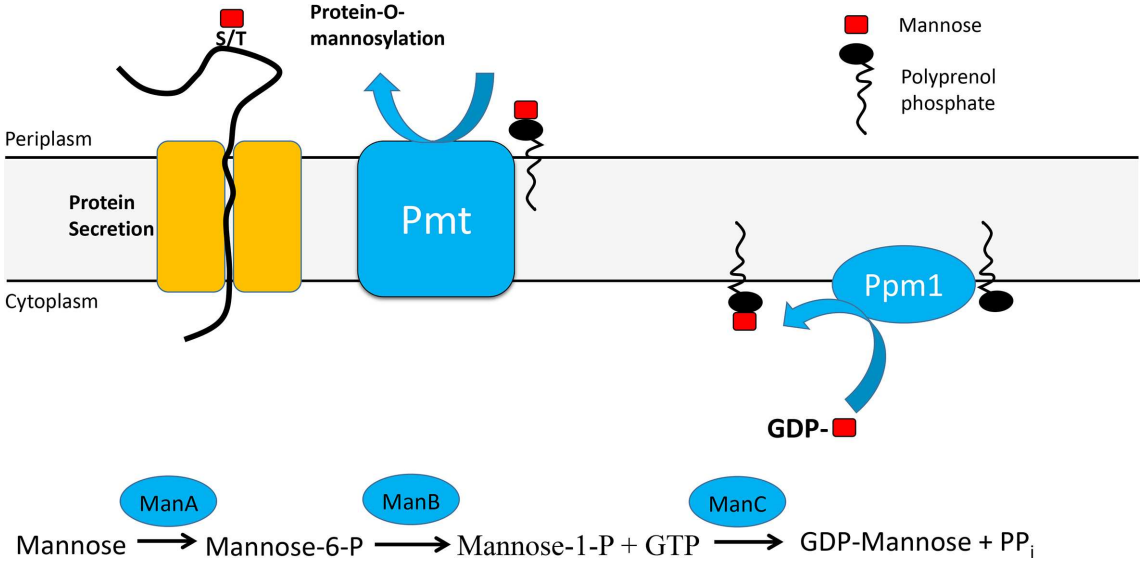

Fig. 1. Model for protein O-mannosylation in *S. coelicolor*. GDP-mannose is synthesised from mannose in consecutive reactions catalysed by ManA, ManB and ManC before transfer of the sugar onto polyprenol phosphate by polyprenol phosphate mannose synthetase (Ppm1). The polyprenol phosphate mannose is flipped to the periplasmic face of the membrane where it is a substrate for Pmt catalysed mannosylation of secreted protein substrates.

coelicolor have greatly increased susceptibility to multiple cell wall targeting antibiotics including vancomycin, daptomycin and *β*-lactams [5, 6]. These strains are also resistant to infection by bacteriophage φC31, indicating that Pmt mediated mannosylation could be required for phage receptor formation [2]. *S. coelicolor ppm1* mutants, and mutants in *manB* and *manC* (Fig. 1) that encode enzymes supplying GDP-mannose to Ppm1, all have similar phenotypes to *pmt*⁻ strains but display more extreme antibiotic sensitivities [5]. PstS was the first, and for many years the only, known target of *S. coelicolor* Pmt mediated mannosylation [7], however the recent characterisation of the *S. coelicolor* membrane glycoproteome led to the identification of thirty-seven novel glycoproteins, with diverse predicted roles including solute binding, polysaccharide hydrolysis, transport, and cell wall biosynthesis [8, 9]. Deletion of the genes encoding either of two of the cell wall active glycoproteins identified in that study, D-Ala-D-Ala carboxypeptidase and an L,D-transpeptidase resulted in strains that were hypersensitive to cell wall targeting antibiotics.

The role of glycoproteins in the maintenance of cell wall integrity is supported by studies in other mircoorganisms. In *Candida albicans*, knockout mutations in *pmt* affect growth, morphogenesis and antifungal resistance [9] while *pmt* knockouts are lethal in *S. cerevisiae*, *S. pombe*, *Aspergillus fumigatus* and *Cryptococcus neoformans* [10–13]. Meanwhile disruption of *pmt* homologues (POMT) in flies [14, 15], mice [16] and humans [17–20] is associated with a number of developmental disorders. Taken together, Pmt/POMT mediated protein O-mannosylation is a fundamentally important protein modification in both prokaryotes and eukaryotes [1].

To gain a deeper understanding of Pmt from *S. coelicolor*, sequence alignments and structural bioinformatics were used to identify candidate residues for an alanine-scanning mutagenesis exploration of structure-activity relationships. In total, we constructed 23 distinct *pmt* mutant alleles and each was assessed for its capacity to complement phage sensitivity and antibiotic hyper-susceptibility phenotypes. Six mutant alleles failed to complement. Modelling suggested that the majority of the corresponding residues are positioned close to the active site and may therefore be involved in substrate binding and or catalysis. Further mutational analysis on each of the six residues showed that strict amino acid conservation is important to preserve function. Purification of membrane fractions and their analysis by Western blotting showed that non-complementing Pmt proteins routinely failed to localize to the membrane. These data show a tight correlation between the activity of Pmt and its stability and/or ability to be correctly localized in the membrane and are suggestive of the existence of a quality control mechanism.

METHODS

Bacterial strains

The genotypes of bacterial strains used in this work are listed in Table S1 (available in the online version of this article). *Streptomyces coelicolor* strains with mutations in *pmt* (DT1025; frameshift from codon Ala121, and DT2008; mutation uncharacterised) are derived from the φC31 sensitive, parent strain J1929 (*pglY*⁻) [21, 22]. *Streptomyces* strains were routinely maintained on mannitol soya (MS) agar at 30 °C and spore stocks were stored in 20% glycerol at −38 °C. The *dam*⁻,

dcm⁻ methylation deficient *E. coli* strain ET12567 (pUZ8002) was used as a donor for plasmid conjugation with *Streptomyces* acceptor strains. *E. coli* DH5α was used for genetic manipulation and propagation of plasmids. *E. coli* strains were routinely grown in LB or on LB containing 0.4% agar.

DNA manipulations

Plasmid DNA was introduced into chemically competent *E. coli* cells by transformation as described previously. Plasmids were purified from *E. coli* using a Spin Miniprep kit (QIAGEN), in accordance with the manufacturer's instructions. Introduction of plasmids into *S. coelicolor* was performed by conjugation [23, 24]. After mixing donor *E. coli* ET12567 (pUZ8002) containing the plasmid to be transferred and recipient *S. coelicolor* spores and plating on mannitol soya flour agar (MSA) +10 mM $MgCl_2$, conjugation plates were incubated at 30 °C for 18 h. Selection for ex-conjugants was performed by overlaying the plates with 1 ml sterile MilliQ H_2O containing 0.5 mg nalidixic acid and 0.5 mg hygromycin. For each conjugation reaction, four ex-conjugant colonies (each representing a biological replicate) were picked after a 7 day incubation, resuspended in water and streaked onto MS agar containing hygromycin (50 μg ml^{-1}). Single colonies from these plates were picked after 7 days at 30 °C, and amplified to generate spore stocks that could be stored at −38 °C in 20% glycerol. *pmt* alleles transferred to *S. coelicolor* by conjugation and integration were validated by PCR and sequencing (Table S2 and GATC Services, Eurofins). Genomic DNA from *Streptomyces* strains was prepared using the CTAB method as described [25].

Plasmid constructions

The plasmids used in this work are all derivatives of the expression vector pIJ10257 [26] in which the wild-type or mutant *pmt* gene is inserted into the NdeI site downstream of the constitutive *ermEp** promoter (Table S3). Plasmids were constructed as follows: DNA fragments were amplified by PCR using primer pairs listed in Table S2 from a J1929 genomic DNA template. To amplify *pmt* and simultaneously introduce a site-directed mutation, two separate PCR reactions were carried out using *S. coelicolor* J1929 genomic DNA as the template. The first reaction contained primer I*pmt*F and a reverse mutagenic primer (such as R82AR) to amplify a fragment comprising the 5′ end of the gene. In the second reaction, the reverse primer I*pmt*R and a forward mutagenic primer (such as R82AF) were used to amplify a fragment comprising the 3′ end of the gene. Phusion Hi-Fidelity Polymerase and a Biometra TProfessional Basic Thermocycler (Thistle Scientific) were used according to the manufacturer's instructions with the following reaction conditions: an initial incubation at 98 °C for 1 min, 30 cycles of 98 °C/10 s, 60 °C/30 s, 72 °C/2 min and finally an incubation at 72 °C for 10 min. The PCR products were digested with DpnI (NEB) to remove template DNA and purified using QIA Quick PCR Purification Kit (QIAGEN). The pairs of amplified products corresponding to each mutant were joined together and cloned into NdeI (NEB) digested pIJ10257 using the In-Fusion HD Cloning Kit (Clontech). Then 5 μl of each reaction product was introduced into chemically competent DH5α *E. coli* by transformation. The restriction endonuclease NdeI and Phusion High-Fidelity DNA Polymerase were obtained from New England Biolabs (NEB).

Conjugation from *E. coli*

The method of intergeneric conjugation was followed as previously described [24].

Antibiotic disc diffusion assay

Approximately 1×10^7 *Streptomyces* spores were evenly spread on a Difco nutrient (DN) agar plate. Sterile filter discs (5 mm width) were prepared from grade 17 chromatography paper (GE Healthcare Whatman) and placed on the plate surface. Then 10 μl of antibiotic stock solution was pipetted on to the disc. Plates were incubated at 30 °C for 36 h and the diameter of the zone of no growth around the disc measured in order to quantify antibiotic susceptibility. Four biological replicates were tested for each strain.

Phage plaque assay

φC31*c*Δ25 is a clear plaque derivative of the temperate phage, φC31 [27]. The phage plaque assay was carried out in accordance with the protocols described [25].

Preparation of *S. coelicolor* membrane fractions

S. coelicolor membrane fractions were isolated as previously described [7, 8, 25]. Briefly, mycelium from *Streptomyces* liquid cultures were grown at 30 °C in Difco nutrient broth (DNB) for 48 h, centrifuged (2 min, 3500 ***g***), washed (20 mM Tris-HCl pH 8, 4 °C) and stored at −80 °C. Mycelial pellets were resuspended in two volumes of lysis buffer (20 mM Tris-HCl pH 8, 4 mM $MgCl_2$, 4 mM DTT containing a protease inhibitor tablet (Roche)). Mycelium was lysed by sonication using a Sonicator 3000 (Misonix) (10 cycles of 30 s pulse and 60 s cooling). Debris was removed by centrifugation (30 min, 5525 ***g*** followed by 30 min at 13500 ***g***, 4 °C). Membranes were finally pelleted by ultracentrifugation (1 h at 100000 ***g***, 4 °C) The membrane pellet was resuspended in 20 mM Tris-HCl pH 8 to yield the membrane fraction while the supernatant constituted the soluble fraction.

SDS-PAGE and Western blotting

Protein concentrations were determined using a Nanodrop 2000 instrument (Thermo Scientific). Membrane and soluble fractions were diluted to ~3 mg ml^{-1} in 1 × RunBlue LDS sample buffer (Expedeon) with β-mercaptoethanol (5% vol/vol), and then incubated at 37 °C for 1 h prior to separation in RunBlue 4–12% gradient SDS protein gels (Expedeon). For protein staining, gels were soaked in InstantBlue protein stain (Expedeon). Proteins were then transferred to 0.45 μm Amersham Hybond PVDF Blotting Membrane (GE healthcare) using the XCell II Blot Module (Invitrogen). Transfer was carried out at 30 V for 1 h. The preparation of the membrane for Western blotting (washing steps and antibody addition) was carried out according to the manufacturer's instructions for the StrepII tag

antibody-HRP conjugate (Novagen). Chemiluminescent substrate for the Western blot was prepared by adding 5 ml of 100 mM Tris-HCl, pH 8.5, buffer with 0.2 mM p-coumaric acid (Sigma) and 1.25 mM luminol to 15 µl of 3% (vol/vol) hydrogen peroxide solution. Under dark room conditions, membranes were incubated with chemiluminescent solution for 1 min. After exposure to the blot, the X-ray film (GE healthcare) was incubated for 1–3 min in developer solution (Kodak) and 30 s in fixer solution (Kodak). The film was rinsed in water and allowed to dry.

Pmt bioinformatics

Pairwise and multiple protein sequence alignments were produced using EMBOSS Needle and Clustal Omega [28, 29]. *S. coelicolor* Pmt homology models were produced using Phyre2 [30], which utilised *Cupriavidus metallidurans* ArnT [31] and *S. cerevisiae* Pmt1-Pmt2 [32] as templates. Protein structures were visualised using CCP4mg [33]. Construct design and sequence trace analysis was carried out using SnapGene (GSL Biotech).

RESULTS AND DISCUSSION

Identification of targets for site-directed mutagenesis

In order to probe structure-function relationships in protein mannosyl transferase from *S. coelicolor*, its sequence was aligned with those of homologues in prokaryotes (*S. griseus*, *M. smegmatis* and *M. tuberculosis*) and eukaryotes (*S. cerevisiae* and *H. sapiens*). The catalytic GT-2 domain is broadly conserved across the prokaryotic and eukaryotic kingdoms (Fig. S1). Twenty-three conserved residues were identified as targets for alanine-scanning mutagenesis: R82, D113, E114, V158, H159, P161, K164, R182, R201, R228, L231, L232, D233, K302, R338, P393, W400, H410, S421, W426, P503, R510, F564. The majority of these residues were targeted on the basis of sequence conservation alone. Some residues, however, are implicated in having a functional role from previous work. These include D113 and E114 which constitute the conserved DE motif, a hallmark of GT-C fold glycosyl transferases [34]. In *S. cerevisiae* Pmt1P, mutation of both homologous residues (Pmt1PD77, Pmt1PE78) led to notable reductions in *in vivo* glycosylation and complete elimination of *in vitro* mannosyl transferase activity [35]. Elsewhere, mutations in the DE motif of *M. tuberculosis* Pmt (Mtb PmtD55, Mtb PmtE56) revealed that the *in vitro* mannosyl transferase activity was reduced, but not completely eliminated [36]. In an earlier study, R138 in *S. cerevisiae* Pmt1P (R182 in *S. coelicolor*) was shown to have an essential role in *in vitro* transferase activity [37]. Finally, in *Cupriavidus metallidurans* ArnT, a lipid A glycosyl transferase, the mutation of D55, K85 and K203 (D113, H159 K302 in *S. coelicolor* respectively) eliminated *in vivo* function [31].

Predicted membrane topology of *S. coelicolor* Pmt

According to TMHMM (Transmembrane Helices; Hidden Markov Model), *S. coelicolor* Pmt is predicted to have 11 transmembrane helices (Figs 2 and S2) ranging in length from 17 to 22 residues. The majority of the 23 residues substituted in this study are predicted to be located in extracellular loop regions. Seven residues (D113, E114, V158, H159, P161, K164 and R182) are predicted to occupy loop 1 and five residues (P393, W400, H410, S421 and W426) are predicted to reside in loop 7. Another four residues (R228, L231, L232 and D233) are on the shorter loop 3 and the beginning of TM4, while residues K302 and R510 occupy loops 5 and 9 respectively (Fig. 2). The hallmark DE motif is located within loop 1, as is universally observed in Pmt homologues across the prokaryotic and eukaryotic kingdoms [34].

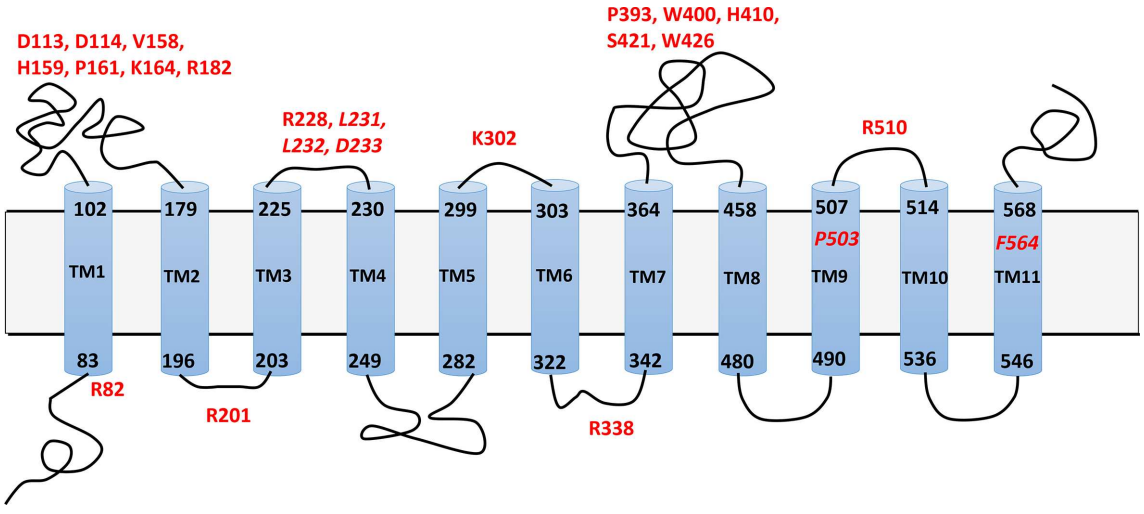

Fig. 2. Protein mannosyl transferase topology model. Predicted membrane topology model for Pmt. The limits of the 11 membrane spanning segments as predicted in TMHMM are specified along with the locations of the residues (red) mutated to alanine in this study. Italics denote mutated residues predicted to be within the transmembrane regions.

Three of the substituted residues are predicted to be located on the cytoplasmic side of Pmt, with R82 in the N-terminal region and residues R201 and R338 located in loops 2 and 6 respectively. Finally, two of the mutated residues are predicted to occupy the transmembrane spanning portion of Pmt, with residues P503 and F564 located on helices 9 and 11 respectively.

The 82 N-terminal residues preceding the first predicted transmembrane helix of *S. coelicolor* Pmt encompass roughly 55 amino acids that are predicted to be intrinsically disordered according to IUPred2A (≥0.5) (Fig. S2c). Moderate peaks in disorder tendency (<0.5) are seen in shorter regions elsewhere.

Identification of conserved residues essential for Pmt function

The twenty-three conserved residues identified above were changed to alanine by site-directed mutagenesis. The activity of Pmts expressed from the twenty-three mutant alleles was then assayed using *in vivo* complementation. Using the integrative vector pIJ10257, *S. coelicolor* wild-type and mutant *pmt* alleles were introduced into the chromosomes of the *pmt* deficient strain DT1025, and the parent strain J1929. DT1025 has a frameshift mutation in *pmt* and is hyper-susceptible to a number of antibiotics compared to its parent, J1929 (Fig. 3, [6]). The antibiotic hypersusceptibility phenotype of DT1025 is complemented by the introduction of a wild-type copy of the *pmt* gene such that the sensitivities to the antibiotics, ampicillin, carbenicillin, vancomycin, imipenem, meropenem, rifampicin and nitrofurantoin are restored to the levels seen in J1929 (Fig. 3) [5]. Six of the twenty-three *pmt* mutant alleles tested failed to complement the antibiotic susceptibility phenotype conferred by the *pmt*$^-$ mutation in DT1025 (Fig. 3). These non-complementing alleles encoded PmtR82A, PmtD113A, PmtH159A, PmtD233A, PmtK302A and PmtR510A. The wild-type (WT) and the seventeen remaining mutant alleles were able to complement DT1025, alleviating the antibiotic susceptibility phenotype (Fig. 3).

As described previously, DT1025 is most susceptible to membrane and cell wall biosynthesis targeting antibiotics, although this strain is also more sensitive to rifampicin, which targets RNA polymerase [6]. As an aside, a greater variety of antibiotics was tested for changes in antibiotic susceptibility. DT1025 was found to have increased susceptibility to nitrofurantoin, an antibiotic that inhibits multiple enzymes that participate in bacterial carbohydrate metabolism, in addition to interfering with cell wall synthesis [38]. DT1025 transformed with the empty plasmid control, and all of the non-complementing mutant strains exhibited very similar levels of susceptibility to antibiotics inhibiting DNA replication (ciprofloxacin, sparfloxacin and mitomycin C) and translation (doxycycline, minocycline, lincomycin, spectinomycin, thiostrepton) as the J1929 parent strain (P<0.05) (Fig. S3), further supporting the envelope-defective nature of the *pmt*$^-$ phenotype.

The complementing and non-complementing DT1025 strains were also tested for other phenotypes of the *pmt*$^-$ mutants, described previously these being resistance to phage φC31 (Fig. 4, Table 1) and a small colony phenotype when grown on Difco Nutrient agar (Fig. S3). DT1025 strains containing the mutant alleles that failed to rescue the DT1025 antibiotic susceptibility phenotype (encoding Pmt with R82A, D113, H159A, D233A, K302A and R510A substitutions) or the empty vector (negative control) showed no evidence of infection by φC31*c*Δ25 within the phage dilution range tested (Fig. 4). The positive control harbouring wild-type *pmt* and the seventeen complemented DT1025 strains from the antibiotic susceptibility assay were vulnerable to phage infection (Fig. 4) and yielded large, clear plaques phenotypically similar to those formed on the J1929 parent strain (not shown). DT1025 strains harbouring *pmt* alleles associated with phage φC31 resistance exhibited slow growth and gave rise to small colonies on DN agar plates (Fig. S4). Thus, all of the strains found to be hypersensitive to antibiotics were also resistant to bacteriophage φC31 infection and exhibited growth defects, while the strains that were complemented for antibiotic hypersusceptibility, without exception, were sensitive to phage φC31 infection and exhibited normal growth rates.

Since DT1025 encodes a frameshift mutation at the codon encoding A121, it is plausible that some of the mutant alleles encode proteins that could interact with this truncated Pmt to yield a functional enzyme. The dominance/recessive nature of the mutations was therefore tested following introduction of the twenty-three mutant *pmt* alleles into the J1929 parent strain. No significant changes in susceptibility of J1929 to any of the antibiotics tested were observed nor was there any change in phage sensitivity/plaque formation (data not shown). These observations indicate that the wt *pmt* allele is dominant and that none of the non-complementing alleles has a dominant negative effect (Table S4).

The ability of the mutant *pmt* alleles to complement a different *pmt*$^-$ mutant strain, DT2008 was also studied [6]. Although the lesion in DT2008 *pmt* remains unknown, DT2008 is fully complemented by addition of a wt *pmt*. If the complementation profiles in DT1025 had been affected by the expression of the truncated endogenous Pmt, the same effect was deemed unlikely to occur in a different genetic background. In addition, our observation that alleles encoding PmtE114A and R182A successfully complemented the *pmt*$^-$ mutation in DT1025 was surprising as homologous residues in *S. cerevisiae* and *M. tuberculosis* Pmts are known to be important for activity [35–37]. We therefore confirmed the consistency of complementation by PmtE114A and PmtR182A and the other alanine variants in the different genetic background of DT2008. The antibiotic susceptibility (Figs S5 and S6) and phage infection (Fig. S7, Table S5) data were fully consistent with those obtained in the DT1025 strains.

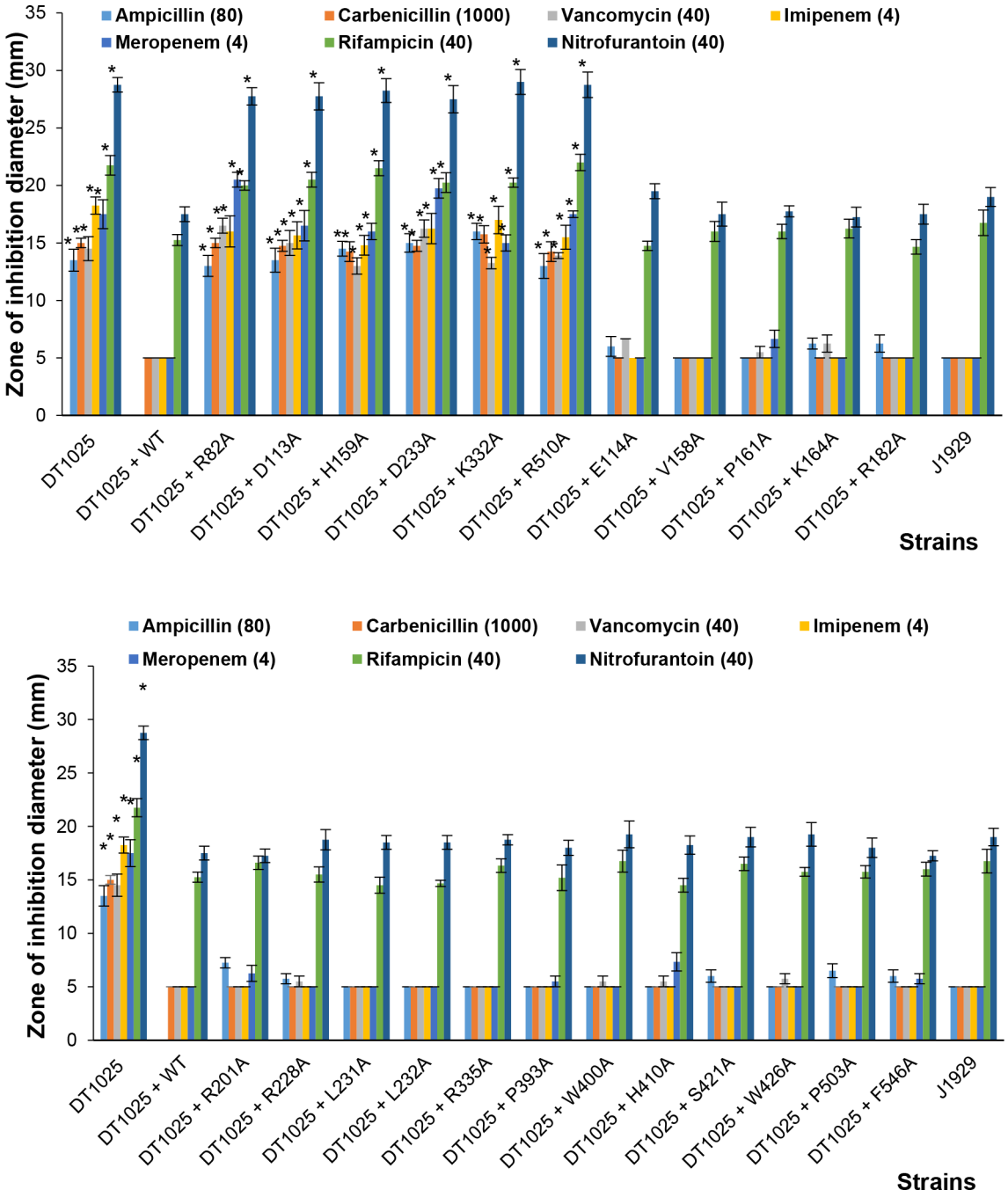

Fig. 3. Antibiotic sensitivity assays for DT1025 transformants. DT1025 strains harbouring genes encoding Pmt variants were assayed for their sensitivity to cell wall/membrane targeting antibiotics, nitrofurantoin and rifampicin. Antibiotic sensitivity was quantified by measuring the zone of inhibition in disc diffusion assays. Shown are the averages of four biological replicates with SEM. The antibiotic paper discs have a diameter of 5 mm, which is shown as the dotted line threshold. The amount of antibiotic used in µg is shown in brackets. The asterisks indicate a $P<0.05$ that the observed differences occurred by chance.

Pmt mutations affect protein abundance and localization

We sought next to establish whether the inability of non-complementing Pmt variants was due to changes in enzyme stability or abundance. To assess the expression levels of the various *pmt* alleles and to determine the protein localization, we used PCR methods to attach a sequence encoding a StrepII tag (WSHPQFEK) upstream or downstream of the coding sequence of the wt *pmt* allele and the six *pmt* mutant alleles that failed to complement the *pmt*⁻ phenotypes.

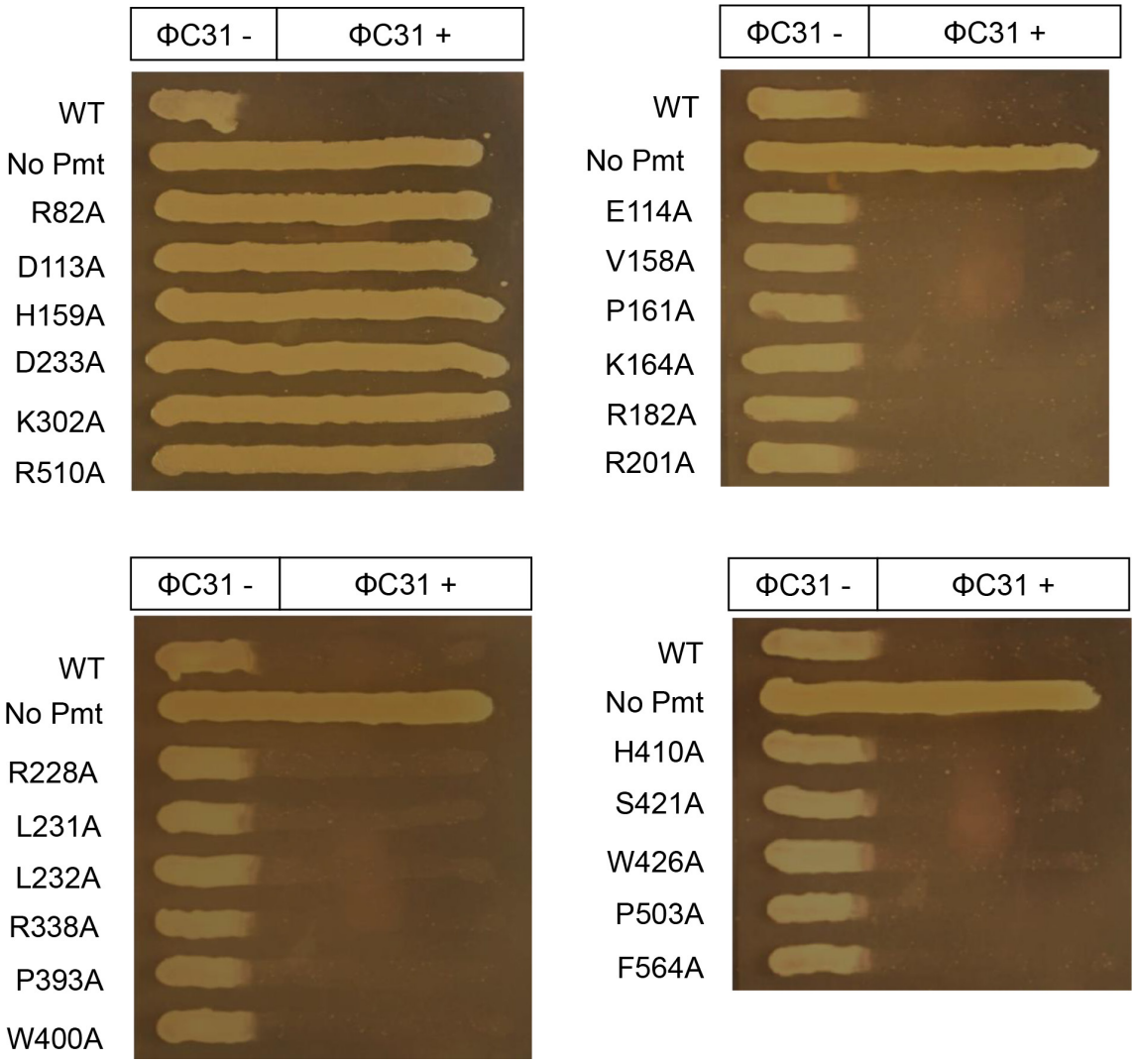

Fig. 4. φC31*c*Δ25 Phage infection assays. DT1025 strains harbouring genes encoding Pmt variants were assayed for their sensitivity to φC31*c*Δ25 phage infection. Phage were plated out on the right side of DN agar plates and spores were subsequently streaked from left to right (from the regions lacking phage to those containing phage). Plates were incubated at 30 °C for 48 h. Images are representative of four biological replicates.

The sequences encoding the N- and C-terminally tagged enzymes were introduced into pIJ10257 and then into the *pmt* deficient strains DT1025 and DT2008. DT1025 and DT2008 containing the wt *pmt* derivatives remained susceptible to φC31*c*Δ25 infection. As expected, upon exposure to φC31*c*Δ25, no plaques were seen for either DT1025 (Table 2) or DT2008 (Table S6) strains encoding the N- and C-terminally tagged Pmt variants (PmtR82A, PmtD113A, PmtH159A, PmtD233A, PmtK302A and PmtR510A) that led to loss of complementation. We conclude that the presence and position of the StrepII tag does not interfere with Pmt function *in vivo*.

An anti-StrepII tag antibody was used to probe for the presence of Pmt by Western blotting of cell fractions that had been resolved by SDS polyacrylamide gel electrophoresis. DT1025 expressing the WT C-terminally StrepII-tagged Pmt yielded a signal for a protein in the membrane fraction with a mobility between those of the 50 and 70 kDa marker proteins (Fig. 5a). As the calculated molecular weight (MW) of StrepII-tagged Pmt is 66 kDa, and because the empty vector control fractions yielded no signal, we conclude this band is Pmt. Surprisingly, none of the six non-functional tagged Pmt variants were detected in either the soluble or membrane fractions of the DT1025 strains (Fig. 5a) or the DT2008 strains (Fig. S8a).

Attempts were made to locate the tagged non-functional Pmt variants in the fractions that had been discarded during cell fractionation. Fractions were taken at intermediate

Table 1. Complemented DT1025 strains are vulnerable to ΦC31 cΔ25 Phage infection. Phage were plated out on DN agar and then SN agar containing spores was added to the top with the plates incubated at 30 °C for 18 h. The average titre is shown ±SEM from four biological replicates. We used 0.1 ml of a 10^{-6} phage stock dilution to obtain countable plaques for phage sensitive strains. Strains that showed no plaques at the lowest phage stock dilution tested (10^{-1}) are represented as having a PFU ml^{-1} $<1\times10^{2}$

Strain	Titre (PFU ml^{-1})
DT1025	$<1\times10^{2}$
DT1025+WT	$(2.63\pm0.14)\times10^{8}$
DT1025+R82A	$<1\times10^{2}$
DT1025+D113A	$<1\times10^{2}$
DT1025+H159A	$<1\times10^{2}$
DT1025+D233A	$<1\times10^{2}$
DT1025+K302A	$<1\times10^{2}$
DT1025+R510A	$<1\times10^{2}$
DT1025+E114A	$(3.21\pm0.29)\times10^{8}$
DT1025+V158A	$(2.12\pm0.09)\times10^{8}$
DT1025+P161A	$(3.13\pm0.14)\times10^{8}$
DT1025+K164A	$(2.37\pm0.12)\times10^{8}$
DT1025+R182A	$(2.56\pm0.36)\times10^{8}$
DT1025+R201A	$(1.74\pm0.07)\times10^{8}$
DT1025+R228A	$(4.12\pm0.42)\times10^{8}$
DT1025+L231A	$(2.28\pm0.23)\times10^{8}$
DT1025+L232A	$(3.48\pm0.37)\times10^{8}$
DT1025+R335A	$(2.32\pm0.18)\times10^{8}$
DT1025+P393A	$(1.94\pm0.27)\times10^{8}$
DT1025+W400A	$(1.82\pm0.08)\times10^{8}$
DT1025+H410A	$(2.67\pm0.13)\times10^{8}$
DT1025+S421A	$(4.34\pm0.34)\times10^{8}$
DT1025+W426A	$(2.59\pm0.25)\times10^{8}$
DT1025+P503A	$(3.56\pm0.27)\times10^{8}$
DT1025+F564A	$(2.71\pm0.07)\times10^{8}$

steps in the differential centrifugation protocol (i. sonication, ii. 5000 ***g*** spin and iii. 15000 ***g*** spin) but no detectable signal for the StrepII tag was obtained by Western blotting (data not shown) implying that the Pmt variant proteins were not present. Genomic DNA from the DT1025 strains was purified and sequences spanning the *pmt* genes at the integration site and at the native locus (including 100 base pairs upstream and downstream) were amplified by PCR. Sequencing of the PCR products in all cases confirmed the presence of the expected *pmt* alleles, the integrity of the integration site, and the absence of any unexpected changes to the DNA sequences (data not shown).

Table 2. The presence of the Strep II Tag does not affect the ability of *pmt* alleles to complement DT1025. ΦC31 cΔ25 phage were plated out on DN agar and SN agar containing spores was overlaid and the plates were incubated at 30 °C for 18 h. The average titre is shown ±SEM from four biological replicates. We used 0.1 ml of a 10^{-6} phage stock dilution to obtain countable plaques for phage sensitive strains. Strains that showed no plaques at the lowest phage stock dilution tested (10^{-1}) are represented as having a PFU ml^{-1} $<1\times10^{2}$

	C-terminal Strep II Tag	N-terminal Strep II Tag
Strain	Titre (PFU ml^{-1})	Titre (PFU ml^{-1})
DT1025	$<1\times10^{2}$	$<1\times10^{2}$
DT1025+WT	$(3.47\pm0.37)\times10^{8}$	$(2.03\pm0.19)\times10^{8}$
DT1025+R82A	$<1\times10^{2}$	$<1\times10^{2}$
DT1025+D113A	$<1\times10^{2}$	$<1\times10^{2}$
DT1025+H159A	$<1\times10^{2}$	$<1\times10^{2}$
DT1025+D233A	$<1\times10^{2}$	$<1\times10^{2}$
DT1025+K302A	$<1\times10^{2}$	$<1\times10^{2}$
DT1025+R510A	$<1\times10^{2}$	$<1\times10^{2}$
DT1025+P160A	$(2.52\pm0.32)\times10^{8}$	$(2.50\pm0.26)\times10^{8}$
DT1025+K164A	$(2.79\pm0.19)\times10^{8}$	$(4.05\pm0.23)\times10^{8}$
DT1025+R228A	$(2.18\pm0.13)\times10^{8}$	$(3.10\pm0.25)\times10^{8}$
DT1025+L231A	$(3.20\pm0.23)\times10^{8}$	$(2.43\pm0.17)\times10^{8}$
DT1025+R335A	$(4.10\pm0.23)\times10^{8}$	$(2.71\pm0.76)\times10^{8}$
DT1025+S421A	$(2.68\pm0.18)\times10^{8}$	$(2.35\pm0.31)\times10^{8}$

The failure to detect the StrepII-tagged Pmt proteins expressed from the six non-complementing *pmt* alleles was surprising given that alanine substitutions normally preserve native protein structure - by simply truncating the residue side-chain they represent a minor perturbation [39]. To test for a potential activity - localisation relationship, Strep II tags were added to a subset of variant Pmts that had complemented the *pmt*⁻ phenotypes in DT1025 and DT2008. Six alleles were chosen encoding PmtP160A, PmtK164A, PmtR228A, PmtL231A, PmtR335A and PmtS421A. StrepII tags were attached to the periplasm facing C-termini using PCR and Infusion cloning, and the recombinant plasmids were introduced into DT1025 and DT2008 via pIJ10257. Phage susceptibility testing showed that all of the resulting strains were vulnerable to phage infection as expected (Tables 2 and S6). Membrane fractions from these strains were purified as described above. Signal corresponding to all of the active Pmt variants was present in the membrane fractions and absent from the soluble fractions from DT1025 (Fig. 5b) and DT2008 strains (Fig. S8b). Moreover, the intensity of the signals obtained and the mobility of the associated proteins was similar to that observed for the wild-type StrepII-tagged Pmt.

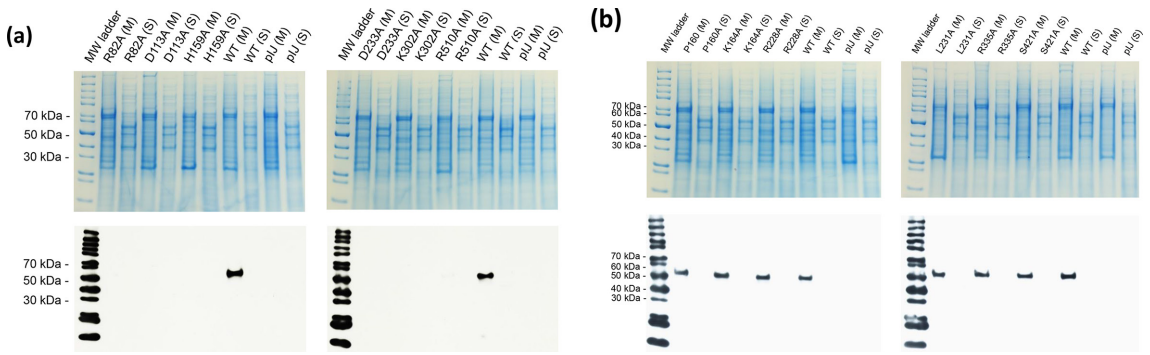

Fig. 5. Expression assays. C-terminal StrepII-tagged Pmt is absent (a) and present (b) in the membrane fractions of DT1025 strains harbouring non-complementing (alanine substitutions at positions 83, 113, 159, 233, 302 and 510) and complementing (alanine substitutions at positions 160, 164, 228, 231, 335 and 421) mutations respectively. Membrane and soluble fractions were loaded onto a 12% SDS-PAGE gel, which was run and stained with Coomassie blue (upper images) to ensure that the protein concentrations in the samples were comparable. After transfer of proteins from an SDS-PAGE gel to a PVDF membrane and washing, the membrane was incubated with a StrepII-Tag Antibody HRP Conjugate, substrate was added and chemoluminescence was detected on an X-ray film (lower image). pIJ: pIJ10257 control, WT: Pmt WT complemented strain control.

Conservative substitutions can abolish Pmt activity

The mutations hitherto described caused substitutions to alanine. Alanine substitution usually preserves protein folding and stability while removing functional groups on side chains [39]. The phenotypes of the strains obtained in the present study were binary with respect to antibiotic and phage susceptibility, resembling either J1929, suggesting the Pmt mutant is fully active or DT1025 (or DT2008) suggesting the Pmt mutant is inactive. We therefore sought to identify partially active Pmts, which would be evidenced by strains with intermediate phenotypes and in which the variant Pmts localise to the cell membrane. We made a set of more conservative mutations at the positions where alanine substitution led to loss of activity. These substitutions were selected variously to preserve charge, polarity and/or size. Thus, R82 was mutated to lysine and histidine; H159 to lysine and asparagine; D233 to glutamate and asparagine; K332 to histidine and arginine; R510 to histidine and lysine; and finally D113 was mutated to glutamate and asparagine. As before, the mutant alleles were cloned into pIJ10257, and subsequently introduced into the *pmt* deficient strain DT1025 by conjugation.

Antibiotic susceptibility tests were carried out to see if an intermediate phenotype had been obtained (Fig. S9). A limited selection of antibiotics was tested: ampicillin, vancomycin, imipenem and meropenem. DT1025 expressing the *pmt* mutants encoding PmtR82K, PmtD113N, PmtD233E complemented the *pmt*⁻ mutation and had similar antibiotic susceptibilities as J1929. The remaining nine strains exhibited antibiotic susceptibilities at levels comparable to the empty plasmid negative control indicating that these *pmt* alleles failed to complement. In phage infectivity assays, a similar profile was observed; three of the 12 strains, those with alleles expressing PmtR82K, PmtD113N and PmtD233E were susceptible to infection by φC31 (Table 3) while the remaining nine alleles failed to complement DT1025 and remained resistant. Finally, expression and localisation experiments with Strep-II tagged derivatives and Western blotting revealed (i) signals corresponding to the expected molecular weight in membrane fractions from strains complemented with alleles encoding PmtR82K, PmtD113N and PmtD233E (Fig. S10) and (ii) the absence of any such signals for the remaining nine alleles/strains. Expansion of the mutant library to include

Table 3. The majority of conservative substitutions yielded *pmt* alleles that could not complement DT1025. ΦC31 cΔ25 phage were plated on DN agar, then SN agar containing spores was added to the top and the plates incubated at 30 °C for 18 h. The average titre is shown ±SEM from four biological replicates. We used 0.1 ml of a 10^{-6} phage stock dilution to obtain countable plaques for phage sensitive strains. Strains that showed no plaques at the lowest phage stock dilution tested (10^{-1}) are represented as having a PFU ml^{-1} <1×10^{2}

Strain	Titre (PFU ml^{-1})
No gene	$<1\times10^{2}$
WT	$(2.20\pm0.69)\times10^{8}$
R82H	$<1\times10^{2}$
R82K	$(2.46\pm0.77)\times10^{8}$
D113E	$<1\times10^{2}$
D113N	$(1.47\pm0.82)\times10^{8}$
H159K	$<1\times10^{2}$
H159N	$<1\times10^{2}$
D233E	$(1.94\pm1.14)\times10^{8}$
D233N	$<1\times10^{2}$
K332H	$<1\times10^{2}$
K332R	$<1\times10^{2}$
R510H	$<1\times10^{2}$
R510K	$<1\times10^{2}$

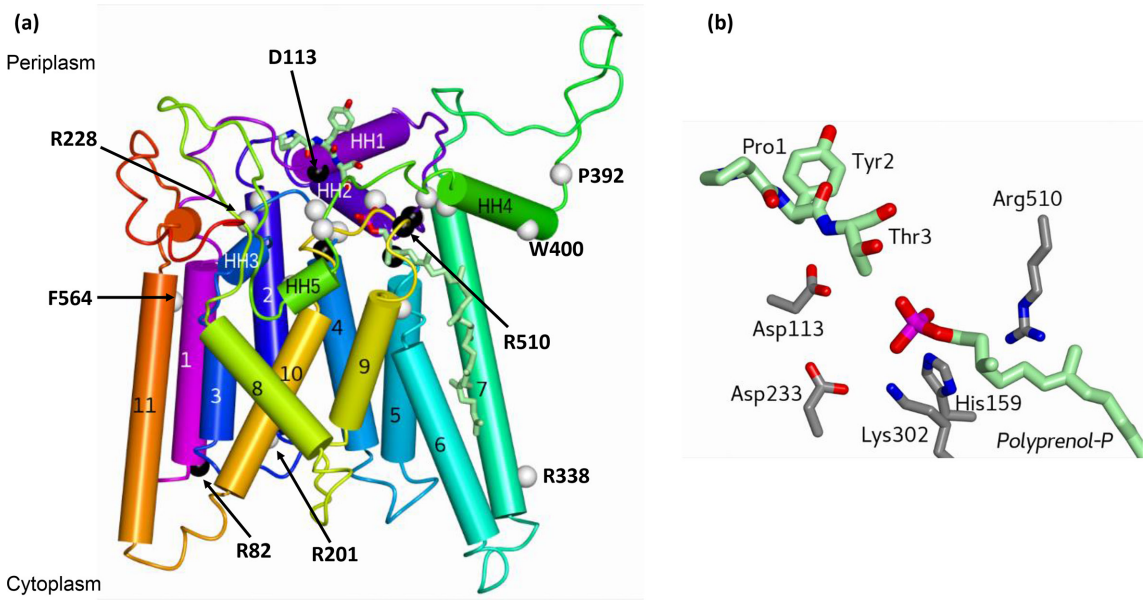

Fig. 6. Phyre2 homology model of *S. coelicolor* Pmt. (a) Worms/tubes rendering of the overall structural model in the programme CCP4mg [33]. The chain is colour ramped from the amino terminus (magenta) to the carboxyl terminus (red). The peptide (Pro-Tyr-Thr) and polyprenol phosphate ligands derived from the *S. cerevisiae* Pmt1-Pmt2 coordinate set (6p25) are displayed in the context of the model following the overlay of protein chains using the 'Superpose models' routine in CCP4mg. Transmembrane helices are numbered 1 to 11 and horizontal helices on the periplasmic face of the membrane are numbered HH1 to HH5. The Cα atoms of residues mutated in this study are displayed as spheres - white for mutations that were associated with complementation of *pmt* deficiency in the *in vivo* assays and black for those that were not. A selection of these residues is labelled. (b) Close-up view of the active site region of the model. The peptide and polyprenol phosphate are displayed in cylinder format with the Cα and side chains of five of the six residues whose mutation to alanine led to loss of complementation of *pmt* deficiency in the *in vivo* assays. Atoms are coloured as follows: nitrogens, blue; oxygens, red; phosphorus, magenta; carbons light green for ligands and grey for protein.

conservative and semi-conservative substitutions therefore failed to break the strict activity-expression/localisation relationship, strengthening the hypothesis that Pmt activity is required for membrane localisation.

A model of *S. coelicolor* Pmt structure based on homology

The Phyre2 Web Portal [30] was used to generate a homology model of *S. coelicolor* Pmt (UNIPROT Q9RKD3). This returned a model containing 445 residues representing 75% of the sequence with 100% confidence using as the top template Chain B (Pmt2) of the protein O-mannosyltransferase Pmt1-Pmt2 complex from *S. cerevisiae* (PDB ID: 6P2R) [32]. The structure of this complex, determined by cryo-EM, reveals structurally similar subunits that form a heterodimer with pseudo two-fold symmetry [32]. The Pmt1 and Pmt2 subunits have 24 and 29% amino acid sequence identity with *S. coelicolor* Pmt. The homology model, shown in Fig. 6 encompasses residues 80–129, 155–257, 280–442 and 457–590. It is in good agreement with the topological predictions made by TMHMM and comprises 11 transmembrane helices, connected by generally shorter segments on the cytoplasmic side and longer segments on the periplasmic face. The missing segments from the model belong to the cytoplasmic domain (residues 1–79) at the N-terminus, the periplasmic segments connecting transmembrane helices TM1/TM2 (residues 130–154) and TM7/TM8 (residues 443–456), and the cytoplasmic segment connecting TM4/TM5 (residues 258–279). Among the residues mutated in this study, Arg82, Arg201 and Arg338 are predicted to be cytoplasm facing with the remaining residues located on periplasmic segments of the polypeptide (Fig. 6a).

Prediction of Pmt enzyme mechanism

In the structure of the yeast Pmt1-Pmt2 complex, a tetrapeptide, Pro-Tyr-Thr-Val, is bound in the acceptor site of Pmt2 while the donor site of Pmt1 is occupied by a molecule of dolichol-phosphate, the reaction product [32]. These ligands are displayed in the context of the *S. coelicolor* model in Fig. 6(a) as part of a superposition that effectively defines the active site. In the course of the Pmt reaction, the hydroxyl group on a serine/threonine side chain of the protein substrate (analogous to Thr3 in Fig. 6b) is activated for nucleophilic attack on the anomeric carbon of the mannose component of PPM. The mannose moiety is not present in the Pmt1-Pmt2 structure but its anomeric carbon (C_1) would be covalently attached to the phosphate of PPM. Analogy with other Pmts implies the reaction proceeds with inversion of stereochemistry at the anomeric carbon so that the covalent linkage to this carbon from the acceptor protein is on the opposite side of the sugar ring to that made to the donor polyprenol-phosphate. As illustrated in Fig. 6(b), five of the six residues whose mutation

to alanine leads to a defective *in vivo* phenotype, are in close proximity to the putative reaction centre. Asp113 is well placed to act as a base in activating the Ser/Thr hydroxyl of the protein substrate. Even though the mannose component is not present in the modelled complex, it is apparent that the side chains of His159, Lys302 and Arg510 are well-placed to orient the phosphate group of the mannosyl-phosphate moiety and facilitate charge transfer onto the phosphate. The remaining 15 periplasm-facing residues, whose mutation to alanine does not lead to a Pmt-defective phenotype in our assays, are further removed or oriented away from the active centre in the modelled structure. Meanwhile Arg82 whose mutation to alanine does cause a defective Pmt phenotype is located at the beginning of TM1 on the cytoplasmic face of the enzyme where it is unlikely to affect catalysis but could conceivably affect stability.

In contrast to alanine, substitutions of PmtD113, PmtD233 and PmtR510 with asparagine, glutamate and lysine respectively yielded active enzymes. The activity of the D113N mutant argues against a role for D113 as a catalytic base since asparagine is not readily ionisable. The loss of activity in the D113E mutant implies precise positioning of the polar side chain may be more important that its charge. Substitutions of the corresponding aspartate residue to glutamate or asparagine in the aminoarabinose transferase, ArnT, from *C. metallidurans* led to loss of function [31]. In the ArnT reaction, the sugar is transferred from a lipid donor to a lipid acceptor in a reaction that leads to cationic antimicrobial peptide resistance. The aspartate of the DE motif aspartate in ArnT acts as a base to activate a nucleophilic phosphate on the lipid A acceptor substrate, rather than activating a serine or threonine hydroxyl as is the case for *S. coelicolor* Pmt.

Only active Pmts appear to be stably expressed and localized

The results of the mutagenesis analysis are readily reconciled with the homology model of *S. coelicolor* Pmt insofar as residues closest to the seat to the transferase reaction exhibited the strongest effects on phenotype in our *in vivo* assays following their substitution by alanine. Curiously, however, we did not observe 'activity-deficient' proteins in Western blots of *S. coelicolor* extracts from strains harbouring the StrepII-tagged Pmt variants, suggesting either that their coding sequences are not being expressed or that the encoded proteins are being produced but then rapidly degraded. It is conceivable that the six point mutants that failed to complement the *pmt*⁻ strains, encode proteins which are prone to misfolding and or aggregation. In *E. coli*, misfolded membrane proteins are degraded by the ATP-dependent zinc metalloprotease FtsH which itself is membrane localized [40]. A homologue of FtsH (Uniprot Q9×814) exists in *S. coelicolor* which may perform a similar function. It is not obvious however, why alanine substitutions of residues R82, D113, H159, D233, K302 or R510 would have such drastic effects on stability. Alanine is considered to be a conservative substitution in structural terms [39] and each of these ionisable residues is expected to be located on the enzyme surface, an expectation consistent with the homology model.

It has been suggested that yeast protein O-mannosyltransferase activity is metal dependent [32] although no active site metal was observed in the Pmt1-Pmt2 crystal structure. This suggestion is based on its structural similarity to the oligosaccharyltransferase, PglB from *Campylobacter lari* [41], in which four side chain carboxylates coordinate an active site Mn^{2+}. Two of these carboxylates participate in the activation of the amide nitrogen of the acceptor asparagine by a twisted amide mechanism. It is conceivable that Pmt from *S. coelicolor* also requires a divalent metal ion for activity. If so, loss of metal coordination induced by mutations such as those introduced here would be a possible explanation for a drastic loss of stability.

CONCLUSION

Across our panel of substitution mutants, complementation of *pmt* deficiency was associated with detectable levels of Pmt protein on Western blots while failure to complement was always associated with the absence of detectable protein. Given the conservative character of the substitutions introduced, we conclude that activity and protein stability/localisation are tightly linked. The molecular basis of this activity-stability relationship remains unknown although one possibility is that mannosylation of one or more Pmt substrates is essential for Pmt stability.

Funding information
This project was funded by the Biotechnology and Biological Sciences Research council UK (project grant reference BB/J016691) and a BBSRC White Rose DTP studentship to NDMH.

Acknowledgements
We are grateful to Professor Mervyn Bibb for providing the expression plasmid, pIJ10257.

Author contributions
The project was conceived by M.C.M.S. and A.J.W., as part of a joint BBSRC studentship within the framework of a long-standing project of M.C.M.S. The experiments were carried out and the data analysed by N.D.M.H., under the supervision of M.C.M.S. and A.J.W. The manuscript was drafted by N.D.M.H., and edited and revised by all authors.

Conflicts of interest
The authors declare that there are no conflicts of interest.

References

1. Lommel M, Strahl S. Protein O-mannosylation: conserved from bacteria to humans. *Glycobiology* 2009;19:816–828.
2. Cowlishaw DA, Smith MCM. Glycosylation of a *Streptomyces coelicolor* A3(2) cell envelope protein is required for infection by bacteriophage phi C31. *Mol Microbiol* 2001;41:601–610.
3. Liu CF, Tonini L, Malaga W, Beau M, Stella A, *et al*. Bacterial protein-O-mannosylating enzyme is crucial for virulence of *Mycobacterium tuberculosis*. *Proc Natl Acad Sci U S A* 2013;110:6560–6565.
4. Mahne M, Tauch A, Puhler A, Kalinowski J. The Corynebacterium glutamicum gene pmt encoding a glycosyltransferase related to eukaryotic protein-O-mannosyltransferases is essential for glycosylation of the resuscitation promoting factor (Rpf2) and other secreted proteins. *FEMS Microbiol Lett* 2006;259:226–233.

5. Howlett R, Anttonen K, Read N, Smith MCM. Disruption of the GDP-mannose synthesis pathway in *Streptomyces coelicolor* results in antibiotic hyper-susceptible phenotypes. *Microbiology (Reading)* 2018;164:614–624.
6. Howlett R, Read N, Varghese A, Kershaw C, Hancock Y, *et al*. *Streptomyces coelicolor* strains lacking polyprenol phosphate mannose synthase and protein O-mannosyl transferase are hyper-susceptible to multiple antibiotics. *Microbiology (Reading)* 2018;164:369–382.
7. Wehmeier S, Varghese AS, Gurcha SS, Tissot B, Panico M, *et al*. Glycosylation of the phosphate binding protein, PstS, in *Streptomyces coelicolor* by a pathway that resembles protein O-mannosylation in eukaryotes. *Mol Microbiol* 2009;71:421–433.
8. Keenan T, Dowle A, Bates R, Smith MCM. Characterization of the *Streptomyces coelicolor* glycoproteome reveals glycoproteins important for cell wall biogenesis. *mBio* 2019;10:e01092-19.
9. Prill SK, Klinkert B, Timpel C, Gale CA, Schroppel K, *et al*. PMT family of *Candida albicans*: five protein mannosyltransferase isoforms affect growth, morphogenesis and antifungal resistance. *Mol Microbiol* 2005;55:546–560.
10. Gentzsch M, Tanner W. The PMT gene family: protein O-glycosylation in *Saccharomyces cerevisiae* is vital. *EMBO J* 1996;15:5752–5759.
11. Willer T, Brandl M, Sipiczki M, Strahl S. Protein O-mannosylation is crucial for cell wall integrity, septation and viability in fission yeast. *Mol Microbiol* 2005;57:156–170.
12. Olson GM, Fox DS, Wang P, Alspaugh JA, Buchanan KL. Role of protein O-mannosyltransferase Pmt4 in the morphogenesis and virulence of *Cryptococcus neoformans*. *Eukaryot Cell* 2007;6:222–234.
13. Mouyna I, Kniemeyer O, Jank T, Loussert C, Mellado E, *et al*. Members of protein O-mannosyltransferase family in *Aspergillus fumigatus* differentially affect growth, morphogenesis and viability. *Mol Microbiol* 2010;76:1205–1221.
14. Ichimiya T, Manya H, Ohmae Y, Yoshida H, Takahashi K, *et al*. The twisted abdomen phenotype of Drosophila POMT1 and POMT2 mutants coincides with their heterophilic protein O-mannosyltransferase activity. *J Biol Chem* 2004;279:42638–42647.
15. Haines N, Seabrooke S, Stewart BA. Dystroglycan and protein O-mannosyltransferases 1 and 2 are required to maintain integrity of Drosophila larval muscles. *Mol Biol Cell* 2007;18:4721–4730.
16. Willer T, Prados B, Falcon-Perez JM, Renner-Muller I, Przemeck GK, *et al*. Targeted disruption of the Walker-Warburg syndrome gene Pomt1 in mouse results in embryonic lethality. *Proc Natl Acad Sci U S A* 2004;101:14126–14131.
17. Taniguchi K, Kobayashi K, Saito K, Yamanouchi H, Ohnuma A, *et al*. Worldwide distribution and broader clinical spectrum of muscle-eye-brain disease. *Hum Mol Genet* 2003;12:527–534.
18. van Reeuwijk J, Janssen M, van den Elzen C, Beltran-Valero de Bernabe D, Sabatelli P, *et al*. POMT2 mutations cause alpha-dystroglycan hypoglycosylation and Walker-Warburg syndrome. *J Med Genet* 2005;42:907–912.
19. van Reeuwijk J, Maugenre S, van den Elzen C, Verrips A, Bertini E, *et al*. The expanding phenotype of POMT1 mutations: from Walker-Warburg syndrome to congenital muscular dystrophy, microcephaly, and mental retardation. *Hum Mutat* 2006;27:453–459.
20. Godfrey C, Clement E, Mein R, Brockington M, Smith J, *et al*. Refining genotype phenotype correlations in muscular dystrophies with defective glycosylation of dystroglycan. *Brain* 2007;130:2725–2735.
21. Bedford DJ, Laity C, Buttner MJ. Two genes involved in the phase-variable phi C31 resistance mechanism of *Streptomyces coelicolor* A3(2). *J Bacteriol* 1995;177:4681–4689.
22. Cowlishaw DA, Smith MC. A gene encoding a homologue of dolichol phosphate-beta-D-mannose synthase is required for infection of *Streptomyces coelicolor* A3(2) by phage (phi)C31. *J Bacteriol* 2002;184:6081–6083.
23. MacNeil DJ. Characterization of a unique methyl-specific restriction system in *Streptomyces avermitilis*. *J Bacteriol* 1988;170:5607–5612.
24. Gust B, Challis GL, Fowler K, Kieser T, Chater KF. PCR-targeted Streptomyces gene replacement identifies a protein domain needed for biosynthesis of the sesquiterpene soil odor geosmin. *Proc Natl Acad Sci U S A* 2003;100:1541–1546.
25. Kieser T, Bibb MJ, Buttner MJ, Chater KF, Hopwood DA. *Practical Streptomyces Genetics*. Norwich: The John Innes Foundation; 2000.
26. Hong HJ, Hutchings MI, Hill LM, Buttner MJ. The role of the novel Fem protein VanK in vancomycin resistance in *Streptomyces coelicolor*. *J Biol Chem* 2005;280:13055–13061.
27. Sinclair RB, Bibb MJ. The repressor gene (c) of the Streptomyces temperate phage phi c31: nucleotide sequence, analysis and functional cloning. *Mol Gen Genet* 1988;213:269–277.
28. Rice P, Longden I, Bleasby A. EMBOSS: the European molecular biology open software suite. *Trends Genet* 2000;16:276–277.
29. Sievers F, Wilm A, Dineen D, Gibson TJ, Karplus K, *et al*. Fast, scalable generation of high-quality protein multiple sequence alignments using Clustal Omega. *Mol Syst Biol* 2011;7:539.
30. Kelley LA, Mezulis S, Yates CM, Wass MN, Sternberg MJ. The Phyre2 web portal for protein modeling, prediction and analysis. *Nat Protoc* 2015;10:845–858.
31. Petrou VI, Herrera CM, Schultz KM, Clarke OB, Vendome J, *et al*. Structures of aminoarabinose transferase ArnT suggest a molecular basis for lipid A glycosylation. *Science* 2016;351:608–612.
32. Bai L, Kovach A, You Q, Kenny A, Li H. Structure of the eukaryotic protein O-mannosyltransferase Pmt1-Pmt2 complex. *Nat Struct Mol Biol* 2019;26:704–711.
33. McNicholas S, Potterton E, Wilson KS, Noble ME. Presenting your structures: the CCP4mg molecular-graphics software. *Acta Crystallogr D Biol Crystallogr* 2011;67:386–394.
34. Lairson LL, Henrissat B, Davies GJ, Withers SG. Glycosyltransferases: structures, functions, and mechanisms. *Annu Rev Biochem* 2008;77:521–555.
35. Lommel M, Schott A, Jank T, Hofmann V, Strahl S. A conserved acidic motif is crucial for enzymatic activity of protein O-mannosyltransferases. *J Biol Chem* 2011;286:39768–39775.
36. VanderVen BC, Harder JD, Crick DC, Belisle JT. Export-mediated assembly of mycobacterial glycoproteins parallels eukaryotic pathways. *Science* 2005;309:941–943.
37. Girrbach V, Zeller T, Priesmeier M, Strahl-Bolsinger S. Structure-function analysis of the dolichyl phosphate-mannose: protein O-mannosyltransferase ScPmt1p. *J Biol Chem* 2000;275:19288–19296.
38. Munoz-Davila MJ. Role of old antibiotics in the Era of antibiotic resistance. Highlighted nitrofurantoin for the treatment of lower urinary tract infections. *Antibiotics (Basel)* 2014;3:39–48.
39. Cunningham BC, Wells JA. High-resolution epitope mapping of hGH-receptor interactions by alanine-scanning mutagenesis. *Science* 1989;244:1081–1085.
40. Karata K, Verma CS, Wilkinson AJ, Ogura T. Probing the mechanism of ATP hydrolysis and substrate translocation in the AAA protease FtsH by modelling and mutagenesis. *Mol Microbiol* 2001;39:890–903.
41. Lizak C, Gerber S, Numao S, Aebi M, Locher KP. X-ray structure of a bacterial oligosaccharyltransferase. *Nature* 2011;474:350–355.

Edited by: R. Manganelli and M. I Hutchings